INTEGRATION OF FULL-WAVEFORM INFORMATION INTO THE AIRBORNE LASER SCANNING DATA FILTERING PROCESS

Y. -C. Lin* and J. P. Mills

School of Civil Engineering and Geosciences, Newcastle University, Newcastle upon Tyne, NE1 7RU, UK - (yu-ching.lin, j.p.mills)@ncl.ac.uk

KEY WORDS: DTM, Filtering, Full-waveform, Laser scanning, Lidar

ABSTRACT

Terrain classification of current discrete airborne laser scanning data requires filtering algorithms based on the spatial relationship between neighbouring three-dimensional points. However, difficulties commonly occur with low vegetation on steep slopes and when abrupt changes take place in the terrain. This paper reports on the integration of additional information from latest generation full-waveform data into a filtering algorithm in order to achieve improved digital terrain model (DTM) creation. Prior to a filtering procedure, each point was given an attribute based on pulse width information. A novel routine was then used to integrate pulse width information into the progressive densification filter developed by Axelsson. The performance was investigated in two areas that were found to be problematic when applying typical filtering algorithms. The derived DTM was found to be up to 0.7 m more accurate than the conventional filtering approach. Moreover, compared to typical filtering algorithms, dense low vegetation points could be removed more effectively. Overall, it is recommended that integrating waveform information can provide a solution for areas where typical filtering algorithms cannot perform well. Full-waveform systems are relatively cost-effective in terms of providing additional information without the need to fuse data from other sensors.

1. INTRODUCTION

Airborne laser scanning (ALS) has been widely adopted to meet the demand for high density and high accuracy digital terrain models (DTMs) in applications such as flood prediction, forest management and landform monitoring (Kenward et al., 2000; McKenna et al., 2008). Prior to digital terrain modelling, separating on-terrain points from off-terrain points, a task commonly referred to as *filtering*, is an essential procedure in processing laser scanning data. However, returns from discrete laser scanning systems alone provide insufficient information about the characteristics of the illuminated surface and, without ancillary imagery, the task of interpreting points presents a considerable challenge (Baltsavias, 1999). Particular problems are encountered in forest areas where ancillary imagery fails to assist in the interpretation of underlying terrain.

Over the past decade there has been a dramatic increase in the development of filtering algorithms which rely strongly on the spatial relationship between points in their pursuit of automated processing (Kraus and Pfeifer, 1998; Axelsson, 1999). Filtering concepts have been categorised into four groups: slope-based, block-minimum, surface-based and clustering / segmentation (Sithole and Vosselman, 2004). Overall, the filters have been found to perform very well in areas with low complexity, such as slightly sloped terrain, sparse vegetation and over small buildings (Sithole and Vosselman, 2004). However, numerous studies have concluded that there are difficulties with classification when using only this geometric information, especially in low, densely vegetated areas, complex urban areas or in terrain with abrupt changes (Flood, 2001; Sithole and Vosselman, 2004). It has therefore been suggested that the integration of additional information with geometry is necessary to improve the reliability of automatic filtering (Ackermann, 1999; Sithole and Vosselman, 2004; Pfeifer and Briese, 2007a). However, whilst ALS intensity data contains information about surface reflectance, and can provide additional information for surface classification and object recognition, it is still rarely used due to its strong variability with several factors, such as spreading loss, surface roughness, object reflectivity, and atmospheric attenuation (Pfeifer and Briese, 2007b). Intensity correction or normalization therefore has to be applied to reduce intensity variation for meaningful comparison to be made between multiple intensity datasets (Kaasalainen et al., 2005; Höfle and Pfeifer, 2007). Additional data sources such as optical and multi-spectral imagery are popularly incorporated with ALS data to improve point identification, for example in the separation of buildings, trees, and grass-covered areas (Suárez et al., 2005; Rottensteiner et al., 2007).

Latest generation small-footprint, full-waveform ALS systems that store the entire waveform of each received pulse have become increasingly available. Received waveforms represent the sum of reflections from all intercepted surfaces within the laser footprint. The shape of waveforms has previously been analysed to achieve improved multi-target resolution and range accuracy (Chauve et al., 2007; Lin et al., 2008). Moreover, waveform parameters such as pulse width, amplitude and backscattered cross-section have been investigated for improving classification. Höfle et al. (2008), for example, found that pulse width and backscatter cross-section have great potential for the classification of tree species and large scale forest characterization. Rutzinger et al. (2008) classified urban vegetation using pulse width and amplitude. Wagner et al. (2008) concluded that pulse width and total cross-section are useful indicators for separating vegetation and terrain. However,

* Corresponding author.

it was also found that the classification of terrain points was difficult in a dense natural forest when using only waveform parameters. Wagner et al. (2008) also questioned whether total cross-section could be used to identify tree species as this parameter was found to vary strongly within the forest canopy. Overall, it is evident that the latest full-waveform systems can provide additional information over discrete return systems. Nevertheless, research on small-footprint, full-waveform ALS systems is still in its infancy. More research efforts, with detailed validation, are required to realise the true potential of full-waveform information for different applications.

According to Wagner et al. (2008), pulse width can be considered as a useful parameter to distinguish between canopy and terrain echoes. However, using only waveform information is still insufficient for high quality DTM generation. In contrast, it has been found that integrating pulse width information into a filtering algorithm can improve digital terrain modelling (Doneus et al., 2008; Wagner et al., 2008). In these studies, the robust interpolation filtering method (Kraus and Pfeifer, 1998; Briese et al., 2002) was chosen to incorporate with pulse width information. However, the potential of this integrated approach has not been widely investigated over different landforms, especially those where traditional filtering algorithms fail to perform well.

The aim of this study was to evaluate the use of pulse width information for improved DTM generation. This paper presents a novel routine to integrate pulse width information into a popular filtering algorithm, namely the progressive densification algorithm by Axelsson (2000). The performance of the approach was assessed over the areas that are considered problematic for typical filtering algorithms. Section Two provides a brief overview of the full-waveform test data. Section Three presents the details of the routine developed for integrating pulse width into Axelsson's filter. Section Four reports the results of a comparison of the developed approach against the original filtering algorithm without using pulse width information. Finally, the main findings of this study are summarised in Section Five.

2. FULL-WAVEFORM TEST DATA

This study utilised data from a Riegl LMS-Q560 full-waveform laser scanner. For each timestamp the transmitted waveform, received waveform and scan angle are stored. The pulse duration (the full width at half maximum amplitude, FWHM) is 4 ns and the sampling rate for digitising the waveform is 1 GHz. The waveform is constructed as an amplitude-against-time dataset. The shape of the transmitted waveform is a Gaussian-like distribution (Wagner et al., 2006). The received waveform is the record of the returned energy from each laser pulse and varies with the height distribution of the illuminated surface. In order to store pulse shape information and offer a parametric description, returned waveforms are popularly modelled by a mathematical function such as the Gaussian function (Wagner et al., 2006; Lin et al., 2008; Reitberger et al., 2008). Therefore, waveform parameters, including amplitude, Gaussian pulse width and Gaussian peak position, can be estimated.

In this study, full-waveform test data were collected over Bristol and Bournemouth in the United Kingdom. The specifications of the two campaigns are shown in Table 1. In terms of footprint size, in Bristol the footprint was three times larger than that in the Bournemouth survey. Both surveys were flown in leaf-on conditions. In order to utilise waveform information, waveform parameters were extracted by applying the rigorous Gaussian detection method reported in Lin et al. (2008). The approach is based on the popular Gaussian decomposition method, but is implemented with rigorous estimates of initial values and a sophisticated iteration procedure. It has demonstrated improved detection results from overlapping and weak pulses, compared to commercial algorithms. It should be noted that the definition of Gaussian pulse width as extracted is not the FWHM value (as previously specified). To clarify, the parameter of pulse width mentioned henceforth represents the Gaussian pulse width extracted from Lin's detection method. It should be noted that a constant factor of 1.665 can be multiplied to convert the extracted Gaussian pulse width into the FWHM.

Table1: Specifications of full-waveform test data

	Bristol	Bournemouth
Date of data acquisition	2nd August, 2006	16th May, 2008
Flying altitude	1000 m	350 m
Scan angle	± 22.5°	± 30°
Nominal footprint size	0.5 m	0.18 m
Mean point density	0.5 points/m^2	15 points/m^2

3. METHODOLOGY

3.1 Background

In previous large- and small-footprint waveform system studies, return pulses from rough surfaces have been found to be broader than the transmitted pulse (Gardner, 1992; Brenner et al., 2003; Wagner et al., 2008). The extracted parameter representing pulse width can therefore be used to evaluate the extent of pulse-broadening to enable a distinction to be made between smooth and rough surfaces. In reality, vegetation is regarded as a rough surface and bare earth terrain is considered to be a relatively smooth surface, therefore implying that pulse width can be a useful indictor in the filtering procedure. However, in small-footprint systems with a size of 0.2 to 2 m, surface information provided by pulse width is considered to be microscale (e.g. height of stones, distribution of tree leaves) and not topographic relief. Local smooth surfaces within a small-footprint could therefore be ground, building roofs, bridges, or tree trunks etc. As a result, it is necessary to combine physical information derived from pulse width with geometric information from three-dimensional coordinates to improve the filtering procedure.

3.2 Point Labelling

Since pulse width can provide additional physical information about 3D points, they can be labelled based on the behaviour of the pulse width and reliability of the estimate of pulse width. The labelling procedure is illustrated in Figure 1. Firstly, any pulse widths extracted from overlapping pulses with a separation of < 6 ns are labelled as Type OV and are considered to be unreliable widths. This is on the basis that when the separation between successive returns is close to 4 ns (the pulse duration), individual returns are partially merged as overlapping pulses (Jutzi and Stilla, 2006; Wagner et al., 2006). In such cases, there is no practicable way to ascertain to what extent the pulse width of overlapping pulses has been contributed to by individual returns. Although the pulse width parameter estimated from Type OV points may not be reliable, precise

geometric information can still be provided. Following this, a threshold value was selected for labelling the remaining points as either smooth (Type A) or rough (Type B) surfaces. The threshold selection was based on simulation results, as described below.

In order to understand the effect of separation distance between successive targets on pulse-broadening, waveforms with returns at close separations were simulated. The pulse was assumed to have a Gaussian distribution with a Gaussian pulse width of 2.6 ns, which was the mean of 12,000 recorded transmitted pulses. The resultant estimates of Gaussian pulse width from simulations are shown in Table 2. For each trial there were 300 simulations and the mean value was calculated. The merged pulses were broader than the transmitted pulse width. With an increase of separation distance and the number of merged targets, pulses displayed an increasing width. The broadened pulses can be deemed as convolutions of the transmitted pulse and height variation of illuminated objects. It should be noted that the simulation results were validated by field procedures. Due to space restrictions, the details regarding this validation are not discussed herein. Since in reality it is not possible to have a perfectly smooth surface as the terrain, based on the simulation results, a pulse width of 2.69 ns was chosen as the threshold to include cases where range separation is within 15 cm. That is to say that a point of interest with a small range separation (< 15 cm) between successive returns is considered to represent a relatively smooth surface. Points with a pulse width of ≤ 2.69 ns were grouped into Type A, which were considered to be smooth surfaces, and therefore potential ground points. Others were grouped into Type B, which were considered to be rough surfaces.

Since the estimate of pulse width from weak pulses is unreliable (Wagner et al., 2006), multiple returns where weak pulses are likely to occur were further categorized into Type MA, which were considered to be obscured smooth surfaces. Remaining points of Type A were categorized into Type SA, which were considered to be open smooth surfaces. As each point was given a label, the filtering procedure could then be considered to be a knowledge-based process.

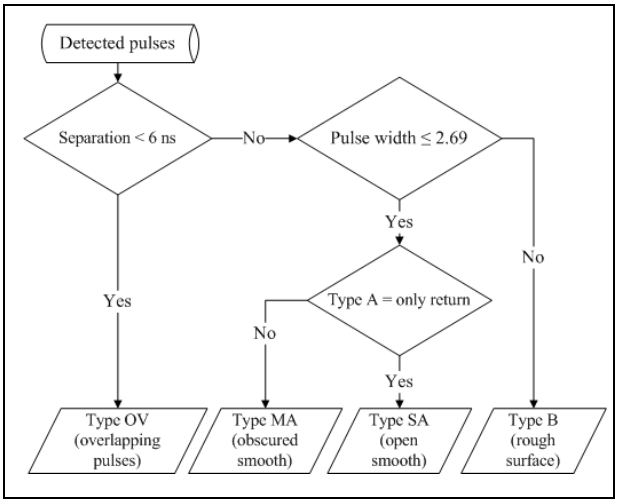

Figure 1: Flowchart for labelling 3D points

Table2: Estimates of pulse width from simulations

No. of successive targets	Separation distance (ns) (1ns=0.15m)	Mean value of pulse width from 300 simulations (ns)
2	3	3.52
2	2	2.99
2	1	2.69
3	2, 2	3.51
3	1, 2	3.06
3	1, 1	2.82

3.3 Filtering

3.3.1 Overview of the progressive densification algorithm

Previous studies into integrating waveform information with filtering algorithms are all based on a surface-based filter, the robust interpolation method (Kraus and Pfeifer, 1998; Briese et al., 2002). In this paper, a progressive Triangulation Irregular Network (TIN) densification developed by Axelsson (2000), was chosen to integrate pulse width information. In an experimental comparison of filter algorithms (Sithole and Vosselman, 2004), this filtering algorithm was considered to perform relatively well, with low total errors.

Axelsson's algorithm starts with a coarse TIN surface made up of seed points which are neighbourhood minima, and then candidate points meeting the threshold criteria are progressively added into the triangulated surface. The criteria are distances to TIN facets and angles to the vertices of the triangle. This algorithm has been embedded in Terrasolid's Terrascan commercial software for ground classification. A set of input parameters need to be assigned by the user, including maximum building size, terrain angle, iteration angle, iteration distance, and maximum edge length. Users can specify the maximum building size parameter to determine the size of area where at least one point is assumed to be a ground point. Such points are then regarded as initial points for ground classification. The terrain angle is the steepest slope angle allowed in the terrain. The maximum edge length refers to the maximum length of the edge of the TIN facets before the iteration angle is reduced. This setting is to avoid unnecessary point density in the ground model. The iteration distance parameter is used to prevent big jumps and is normally set to between 0.5 and 1.5 m. Also, a small angle of close to 4.0 degrees in flat terrain, and a bigger angle of close to 10.0 degrees in hilly terrain are suggested in the TerraScan user's guide (Terrasolid, 2005). It is required that users adjust these parameters to suit different topography. However, without information concerning the points of interest, the "control" of the eagerness of the algorithm to include points when building terrain models becomes challenging. For example, the higher the iteration angle, the more eager the algorithm will be to include either hills or vegetation points, which are unlikely to be identifiable in discrete ALS data. Conversely, if such information could be provided, for example by waveform parameters, this "control" becomes target (vegetation or terrain) specific. As a result, it would be possible to improve the filtering process, based on the integration of geometric and physical information in relation to the 3D points.

3.3.2 Integration of pulse width information

Since 3D points had been labelled based on pulse width information, as described in Section 3.2, a point has possible surface information attributed to it. A novel routine to integrate such information into Axelsson's progressive densification algorithm is proposed in Table 3. The aim was to achieve high

quality filtering whilst minimising the effort required to change parameter settings for different types of topography.

Since in reality, it is not feasible for a laser pulse to always reach the ground, it is reasonable to assume that the lowest points within a large grid cell are ground points at the initial stage. In the first step, an initial ground surface was created by selecting the lowest points from all types of points within areas of 50 m x 50 m and iteratively adding their neighbours with small height (iteration distance 0.5 m) and small angle (iteration angle 0.5°) differences. The ground points selected from the first step generated an initially coarse ground surface. Moreover, in each step, a terrain angle of 88° is used to allow various landforms to be considered. Since points of Type MA were likely to be underlying terrain in forest areas, a high iteration angle (10°) and a large iteration distance (1.5 m) were applied to densify the ground model derived from the previous step. Following this, the clustering of Type SA has to be checked (i.e. validate the homogeneity of the estimate of pulse width in the neighbourhood) to ensure Type SA points are potential ground points. It was assumed that Type SA points, which were considered to be on open terrain, should be close to other points with the same characteristic pulse width. Therefore, if three or more Type SA points are found within an area with a specified diameter, then the point of interest remains as Type SA. Points failing to pass this check are removed from Type SA. Finally, Type SA points with specified thresholds (defined later) were included to densify the ground model. Since points reflected from open ground surfaces should have small height differences due to the short distance to neighbouring points, a low iteration distance (0.5 m) was applied to Type SA points. In addition, a large iteration angle (10°) and a small value (1 m) for maximum edge length were applied to include possible terrain with abrupt changes.

Table 3: Filtering routine steps with pulse width information

Step	Input type	Max. Bldg (m)	Terrain angle (°)	Iteration angle (°)	Iteration distance (m)	Max edge (m)
1	all	50	88	0.5	0.5	5
2	MA	-	88	10	1.5	5
3	SA	Clustering check. (Points failing to pass this check are removed from Type SA).				
4	SA	-	88	10	0.5	1

4. RESULTS

Sithole and Vosselman (2004) compared several filters and found that discontinuities (e.g. break-lines) and ramps were the most difficult types of terrain to perform correct filtering. Interestingly, such failures are present where Type I errors (reject bare-Earth points) occur, such as the top edge of discontinuities or both the top and bottom edges (Sithole and Vosselman, 2004) . The same failure has also been highlighted by several other studies (Huising and Pereira, 1998; Zhang and Whitman, 2005). In other words, such areas tend to be incorrectly removed by typical filtering algorithms, resulting in missing terrain detail. On the other hand, several previous studies have pointed out that terrain covered by low vegetation is a difficult case, and thus generates an overestimated terrain surface (Pfeifer et al., 2004). Therefore, in order to assess the developed routine, one area of terrain with abrupt changes and one with low vegetation, which are considered to be problematic for typical filtering algorithms, were examined.

An area with two artificial mounds in the Bournemouth dataset, which was considered to be representative of "discontinuous" terrain, was investigated (see Figure 2). The performance of the developed approach was compared with Axelsson's algorithm with an iteration angle of 6°, iteration distance of 1.5 m and maximum edge length of 5 m. Kriging interpolation was applied to create grid DTMs with 0.5 m and 1 m cell sizes for the Bournemouth and Bristol datasets respectively. As shown in Figure 3, the DTM created using pulse width information was found to be above that created without pulse width information. In addition, the edge of the mounds, and some details of their tops, was missing from the DTM generated using standard filtering (Figure 4). The height difference between the two DTMs was up to 0.70 m on the bigger mound and ~ 0.25 m on the smaller mound. Further, with a change of iteration angle up to 10°, a height difference of 0.45 m still occurs. It is therefore evident that using the filter without pulse width information has seriously underestimated terrain height in this example.

A dense, low vegetation area in the Bristol dataset was also examined (see Figure 5). As shown in Figure 6, filtering without pulse width information incorrectly includes more low vegetation points. In this case the height difference between the two DTMs was found to be up to 2.8 m. Such filtering error causes the overestimate of terrain height and incorrect representation of terrain surface. In contrast, using pulse width information generates a relatively smooth DTM, with the correct filtering of low vegetation. However, some positive height differences occurred in tree-covered areas, where the DTM created using pulse width information is found to be above that generated without the information. Further field validation is required to confirm whether rough underlying terrain was actually present in such areas or not. Moreover, since real terrain points underlying vegetation might be very sparse, a trade-off between classification and accuracy has to be determined. For example, if there are no real terrain points in a dense forest area, low vegetation points close to the ground might be better considered for inclusion in DTM generation. Otherwise terrain heights estimated by interpolation algorithms may generate greater errors than those created by including low vegetation points.

This study was based on the Axelsson filter that focuses on minimizing Type I errors (reject bare-Earth points). Compared to other filters, this filter was found to produce more Type II errors (accept object points) (Sithole and Vosselman, 2004). Since analysis of pulse width can provide information about the illuminated surface, integrating pulse width information into Axelsson's filter can greatly minimize Type II errors. The preliminary results presented here have demonstrated that the developed routine, which is based on the knowledge of pulse width, can include as many terrain points as possible and also avoid including off-terrain points.

5. CONCLUSIONS

This study set out to investigate whether information derived from the latest generation full-waveform, small-footprint airborne laser scanning data could improve digital terrain modelling. A novel routine was designed to integrate waveform information into a commonly used filtering algorithm. The preliminary results have demonstrated that integrating pulse width information can provide a solution for areas where conventional filtering algorithms cannot perform well. On the top of an artificial mound, points rejected (Type I error) by a

typical filtering algorithm can be correctly included in the developed routine. More low vegetation can also be correctly removed. However, rough or steep terrains with low vegetation cover, as well as forest terrain, still require further investigation and detailed validation. In addition, although identifying vegetation points becomes easier with the help of waveform information, it may be the case that in some densely vegetated areas insufficient "true" ground points exist for high-resolution DTM generation. In such cases, it might still be better to assume that the lowest point within a specified or adaptive window size is a ground point.

The performance of existing filtering algorithms depends on the type of landscape (Sithole and Vosselman, 2004). Such approaches may require that users determine which type of landscape is being processed and then specify optimal parameters. As demonstrated in this paper, by using waveform information it is possible to automatically determine the landscape characteristics and then use the optimal parameter set for that specific landscape type. This will improve the automation of filtering procedures since less effort is required by users. Moreover, compared to ALS intensity values, pulse width information is easier to apply to different surveys since neither prior calibration or normalization procedures are required. Using full-waveform ALS data provides valuable physical and geometric information simultaneously. Such systems are relatively cost-effective in terms of providing multiple-information without the need to fuse data from other sensors.

Figure 2: Examined area with artificial mounds

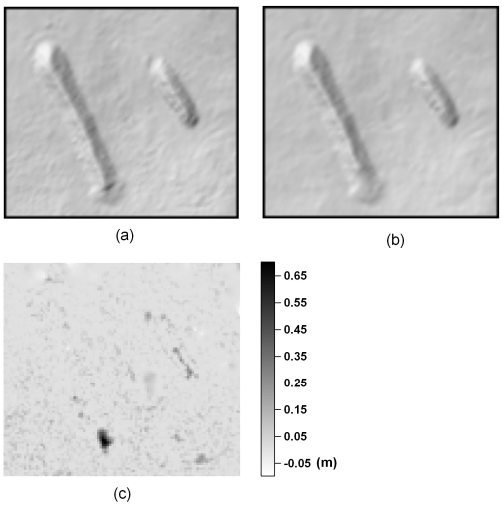

Figure 3: Filtering results in a mound area. (a): DTM from the developed routine with the integration of pulse width information, (b): DTM without pulse width information (c): height difference map between (a) and (b).

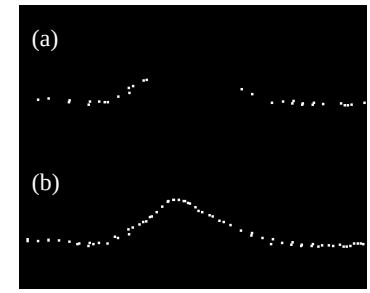

Figure 4: Section view of a mound extracted using the filter (a) without pulse width information and (b) with pulse width information.

Figure 5: Examined low vegetated area

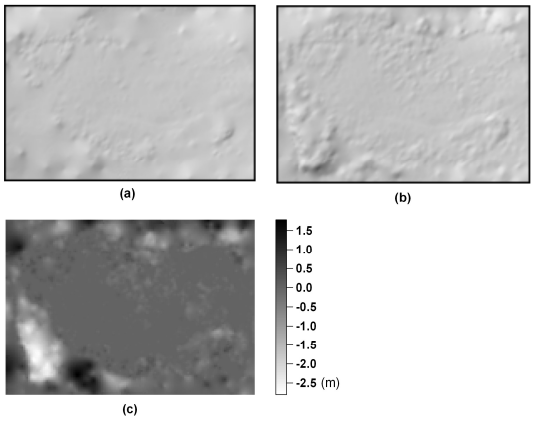

Figure 6: Filtering results in low vegetation area. (a): DTM from the developed routine with the integration of pulse width information, (b): DTM without pulse width information (c): height difference map between (a) and (b).

ACKNOWLEDGEMENTS

The authors would like to thank Ordnance Survey for providing airborne laser scanning data and support during this research programme. The authors are also grateful to 3D Laser Mapping, UK, and RIEGL, Austria, for acquisition of full-waveform airborne laser scanning data and the provision of associated processing software.

REFERENCES

Ackermann, F., 1999. Airborne laser scanning - present status and future expectations. ISPRS Journal of Photogrammetry & Remote Sensing, 54: 64-67.

Axelsson, P., 1999. Processing of laser scanner data—algorithms and applications. ISPRS Journal of Photogrammetry & Remote Sensing, 54: 138-147.

Axelsson, P., 2000. DEM generation from laser scanner data using adaptive TIN models. International Archives of Photogrammetry, Remote Sensing and Spatial Information Sciences, 33(B4/1): 110-117.

Baltsavias, E.P., 1999. A comparison between photogrammetry and laser scanning. ISPRS Journal of Photogrammetry & Remote Sensing, 54: 83-94.

Brenner, A.C., Zwally, H.J., Bentley, C.R., Csatho, B.M., Harding, D.J., Hofton, M.A., Minster, J.-B., Roberts, L., Saba, J.L., Thomas, R.H. and Yi, D., 2003. Geoscience Laser Altimeter System (GLAS) - derivation of range and range distributions from laser pulse waveform analysis for surface elevations, roughness, slope, and vegetation heights. http://www.csr.utexas.edu/glas/atbd.html [Accessed: 12 March, 2009].

Briese, C., Pfeifer, N. and Dorninger, P., 2002. Applications of the robust interpolation for DTM determination. International Archives of the Photogrammetry, Remote Sensing and Spatial Information Sciences, 34(Part 3A): 55-61.

Chauve, A., Mallet, C.e., Bretar, F.e.e., Durrieu, S., Deseilligny, M.P. and Puech, W., 2007. Processing full-waveform lidar data: modelling raw signals. International Archives of the Photogrammetry, Remote Sensing and Spatial Information Sciences, 36(3/W52): 102-107.

Doneus, M., Briese, C., Fera, M. and Janner, M., 2008. Archaeological prospection of forested areas using full-waveform airborne laser scanning. Journal of Archaeological Science, 35(4): 882-893.

Flood, M., 2001. Lidar activities and research priorities in the commercial sector. International Archives of the Photogrammetry, Remote Sensing and Spatial Information Sciences, 34(3/W4): 3-7.

Gardner, C.S., 1992. Ranging performance of satellite laser altimeters. IEEE Transactions on Geoscience and Remote Sensing, 30(5): 1061-1072.

Höfle, B., Hollaus, M., Lehner, H., Pfeifer, N. and Wagner, W., 2008. Area-based parameterization of forest structure using full-waveform airborne laser scanning data. SilviLaser 2008, September 17-19, 2008, Edinburgh, UK.

Höfle, B. and Pfeifer, N., 2007. Correction of laser scanning intensity data: Data and model-driven approaches. ISPRS Journal of Photogrammetry and Remote Sensing, 62(6): 415-433.

Huising, E.J. and Pereira, L.M.G., 1998. Errors and accuracy estimates of laser data acquired by various laser scanning systems for topographic applications. ISPRS Journal of Photogrammetry & Remote Sensing, 53(5): 245-261.

Jutzi, B. and Stilla, U., 2006. Range determination with waveform recording laser systems using a Wiener Filter. ISPRS Journal of Photogrammetry & Remote Sensing, 61(2): 95-107.

Kaasalainen, S., Ahokas, E., Hyyppa, J. and Suomalainen, J., 2005. Study of surface brightness from backscattered laser intensity: calibration of laser data. Geoscience and Remote Sensing Letters, IEEE, 2(3): 255-259.

Kenward, T., Lettenmaier, D.P., Wood, E.F. and Fielding, E., 2000. Effects of digital elevation model accuracy on hydrologic predictions. Remote Sensing of Environment, 74(3): 432-444.

Kraus, K. and Pfeifer, N., 1998. Determination of terrain models in wooded areas with airborne laser scanner data. ISPRS Journal of Photogrammetry & Remote Sensing, 53(4): 193-203.

Lin, Y.-C., Mills, J. and Smith-Voysey, S., 2008. Detection of weak and overlapping pulses from waveform airborne laser scanning data. SilviLaser 2008, September, 17-19, 2008, Edinburgh, UK.

McKenna, J.P., Lidke, D.J. and Coe, J.A., 2008. Landslides mapped from LIDAR imagery, Kitsap County, Washington. U.S. Geological Survey Open-File Report 2008-1292, 81.

Pfeifer, N. and Briese, C., 2007a. Geometrical aspects of airborne laser scanning and terrestrial laser scanning. International Archives of the Photogrammetry, Remote Sensing and Spatial Information Sciences, 36(3/W52): 311-319.

Pfeifer, N. and Briese, C., 2007b. Laser scanning - principles and application, III International Scientific Conference. Geo-Sibir, Nowosibirsk, 93-112 p.

Pfeifer, N., Gorte, B. and Elberink, S.O., 2004. Influences of vegetation on laser altimetry - analysis and correction approaches. International Archives of the Photogrammetry, Remote Sensing and Spatial Information Sciences, 36(8/W2): 283-287.

Reitberger, J., Krzystek, P. and Stilla, U., 2008. Analysis of full waveform LIDAR data for the classification of deciduous and coniferous trees. International Journal of Remote Sensing, 29(5): 1407 - 1431.

Rottensteiner, F., Trinder, J., Clode, S. and Kubik, K., 2007. Building detection by fusion of airborne laser scanner data and multi-spectral images: Performance evaluation and sensitivity analysis. ISPRS Journal of Photogrammetry and Remote Sensing, 62(2): 135-149.

Rutzinger, M., Höfle, B., Hollaus, M. and Pfeifer, N., 2008. Object-based point cloud analysis of full-waveform airborne laser scanning data for urban vegetation classification. Sensors, 8: 4505-4528.

Sithole, G. and Vosselman, G., 2004. Experimental comparison of filter algorithms for bare-Earth extraction from airborne laser scanning point clouds. ISPRS Journal of Photogrammetry & Remote Sensing, 59(1-2): 85-101.

Terrasolid, 2005. TerraScan user's guide. http://cdn.terrasolid.fi/tscan.pdf [Accessed: 20 Feb, 2009].

Suárez, J.C., Ontiveros, C., Smith, S. and Snape, S., 2005. Use of airborne LiDAR and aerial photography in the estimation of individual tree heights in forestry. Computers & Geosciences, 31(2): 253-262.

Wagner, W., Hollaus, M., Briese, C. and Ducic, V., 2008. 3D vegetation mapping using small-footprint full-waveform airborne laser scanners. International Journal of Remote Sensing, 29(5): 1433-1452.

Wagner, W., Ullrich, A., Ducic, V., Melzer, T. and Studnicka, N., 2006. Gaussian decomposition and calibration of a novel small-footprint full-waveform digitising airborne laser scanner. ISPRS Journal of Photogrammetry & Remote Sensing, 60: 100-112.

Zhang, K. and Whitman, D., 2005. Comparison of three algorithms for filtering airborne lidar data. Photogrammetric Engineering & Remote Sensing, 71(3): 313-324.